ELSEVIER

www.elsevier.nl/locate/jorganchem

Journal of Organometallic Chemistry 588 (1999) 51–59

Journal of Organometallic Chemistry

# Synthesis and characterization of sterically hindered arylsilanes containing the 2,4,6-trimethoxyphenyl ligand (TMP): X-ray structures of $(TMP)SiH_3$, $(TMP)_2SiH_2$, and $(TMP)_3SiH$

Janet Braddock-Wilking *, Yanina Levchinsky, Nigam P. Rath

*Department of Chemistry, University of Missouri–St. Louis, 8001 Natural Bridge Road, St. Louis, MO 63121, USA*

Received 9 April 1999

**Abstract**

The homologous series of primary, secondary and tertiary silanes containing the sterically demanding 2,4,6-trimethoxyphenyl (TMP) group have been prepared in yields ranging from 22 to 45%. The arylsilanes were characterized by multinuclear NMR, IR, GC–MS, elemental analyses, and X-ray crystallography. Relatively short intramolecular distances are observed between Si and the O atoms in the *ortho*-methoxy groups of the aryl ligand and are shorter than the sum of the van der Waal's radii in the solid state for all three arylsilanes. 

*Keywords:* Silicon; Arylsilane; Steric hindrance; Solid state structure

## 1. Introduction

Sterically hindered ligands are known to stabilize coordinatively unsaturated molecules, especially those involving main group elements [1]. In addition, the steric encumbrance provided by such groups can result in unusual bonding environments. Recently, we reported the synthesis and characterization of a number of sterically hindered diarylsilanes containing Mes (Mes = 2,4,6-trimethylphenyl) and $R_F$ ($R_F$ = 2,4,6-tris(trifluoromethyl)phenyl) substituents [2]. The latter system exhibited unusual intramolecular interactions in the solid state.

In a continuation of our study of sterically hindered arylsilanes, we have prepared mono-, di-, and triarylsilanes containing the bulky and electron-rich 2,4,6-trimethoxyphenyl (TMP) substituent. The TMP ligand contains O-donor atoms attached at the *ortho*-position of the aromatic ring and provides the potential for intramolecular interactions. Hydrosilanes containing substituents that participate in intramolecular interactions with the Si center are of interest, especially in the enhanced reactivity of the Si–H bond compared with that of normal hydrosilanes [3]. Herein, we report the synthesis, spectroscopic and X-ray crystal structure determination of $(TMP)SiH_3$ (**1**), $(TMP)_2SiH_2$ (**2**), and $(TMP)_3SiH$ (**3**).

## 2. Results and discussion

Hydrosilanes are synthetically useful precursors for the preparation of other silicon compounds such as halosilanes [4], transition metal silyl complexes [5], and oligo- and polysilanes (through transition-metal-catalyzed dehydrocoupling) [6]. Unfortunately, not very many sterically demanding hydrosilanes (primary, secondary, or tertiary) are commercially available but they can be prepared by relatively simple synthetic procedures.

Significant interest has been expressed in the use of the 2,4,6-tris(trifluoromethyl)phenyl group ($R_F$) as a sterically demanding group for the stabilization of low-valent main group compounds [7]. The $R_F$ ligand provides a unique blend of stabilizing features: steric shielding, electron-withdrawing capability due to the $CF_3$ groups, and electron-donating ability via the lone pairs on the fluorine atoms in the *ortho*-$CF_3$ positions.

* Corresponding author. Tel.: +1-314-5166436; fax: +1-314-5165342.

*E-mail address:* wilking@jinx.umsl.edu (J. Braddock-Wilking)

0022-328X/99/$ - see front matter 
PII: S0022-328X(99)00345-9

A related sterically hindered aryl group capable of all of the stabilizing features found with the $R_F$ *but* with electron-donating groups can be found in the 2,4,6-trimethoxyphenyl substituent (TMP). This ligand should have roughly the same steric size as the $R_F$ and mesityl groups but is more electron-rich as illustrated by the triarylphosphine $P(TMP)_3$ which is a highly basic phosphine due to the presence of the TMP substituents [8].

### 2.1. Synthesis of 2,4,6-trimethoxyphenyl-substituted hydrosilanes

Compounds **1**–**3** were prepared by the synthetic route shown in Scheme 1. Direct metallation of 1,3,5-trimethoxybenzene with *n*-BuLi (in THF or DME) afforded the aryllithium reagent, (TMP)Li [9]. Reaction of the appropriate number of equivalents of (TMP)Li with $HSiCl_3$ in $Et_2O$ provided the intermediate chlorosilanes. The mono- and diarylchlorosilanes were reduced with $LiAlH_4$ (in $Et_2O$) to provide the desired hydrosilane.

Compounds **1**–**3** were isolated as white crystalline solids in yields ranging from 22 to 45% after an aqueous workup. Recrystallization from either $Et_2O$ or $Et_2O$/pentane solutions provided X-ray-quality crystals of **1**–**3**. In addition, compounds **1**–**3** were characterized by multinuclear NMR, IR, mass spectrometry and elemental analyses. A summary of the $^1H$ and $^{29}Si\{^1H\}$ chemical shifts, and Si–H stretching frequencies (IR), melting points, and analyses data, for **1**–**3** is given in Table 1.

In all the reactions using $HSiCl_3$, a significant amount of (TMP)H was always observed. This is a notable problem for the synthesis of $(TMP)SiH_3$ since these two compounds are difficult to separate from each other due to similar GC retention times and solubilities. The formation of large amounts of (TMP)H is believed to be due to reaction of (TMP)Li with the acidic proton in $HSiCl_3$ [10]. Compound **1** was obtained in a slightly higher yield when prepared from $SiCl_4$ and (TMP)Li followed by reduction with $LiAlH_4$. Unlike the reaction using $HSiCl_3$ as the silicon precursor, the reaction with $SiCl_4$ displayed a number of color changes (source not identified). However, a smaller amount of (TMP)H was formed (probably due to cleavage of the TMP group at silicon by $LiAlH_4$) making the separation of the starting material from $(TMP)SiH_3$ easier. An analytical sample of $(TMP)SiH_3$ was obtained by repeated fractional crystallization. The use of $SiCl_4$ for the preparation of either $(TMP)_2SiH_2$ or $(TMP)_3SiH$ was unsuccessful. In contrast to the Mes and $R_F$ systems [2], attempts to make $H_3Si(TMP)$ from $H_3Si(OTf)$ and (TMP)Li resulted in exclusive formation of (TMP)H.

The Si–H resonance in the $^1H$-NMR spectrum for compounds **1**–**3** appear at increasing frequency as aryl substitution at silicon increases with resonances at $\delta$ 4.59, 5.61, and 6.36 ppm ($C_6D_6$) for **1**, **2**, and **3**, respectively [11]. A positive shift is also seen in the $^{29}Si\{^1H\}$-NMR spectrum for increased aryl substitution in compounds **1**–**3**: $\delta$ −80.0 for **1**, −67.6 for **2**, and −54.7 ppm for **3**. The presence of the Si–H unit in **1**–**3** is also confirmed by the medium to strong Si–H stretching bands near 2200 $cm^{-1}$ in the infrared spectrum.

In order to optimize yields, several experiments were performed to determine the best conditions for the preparation of (TMP)Li from deprotonation of (TMP)H by *n*-BuLi followed by quenching with $CD_3OD$ to give (TMP)D. Three different solvents [DME, $Et_2O$ (reflux for 24 h only), and THF] were employed at room temperature or at reflux from 2–24 h. Analysis by $^{13}C$-NMR and mass spectrometry (EI) showed that the highest yield of (TMP)D was obtained at room temperature in THF or DME after 2 h (94%) [12]. Van Koten and coworkers observed by NMR spectroscopy exclusive formation of (TMP)D [from (TMP)H and *n*-BuLi in $Et_2O$ for 70 h at room temperature followed by quenching with $D_2O$] [9a]. In contrast to the high yields obtained by these authors, only minor yields of products were obtained in $Et_2O$ at room temperature in the current study.

### 2.2. X-ray crystal structure analysis of compounds 1–3

The structures of **1**–**3** were confirmed by single-crystal X-ray diffraction. The molecular structures along with the atom-numbering scheme are shown in Figs. 1–3, respectively and selected bond lengths and angles are given in Table 2. Selected nonbonded O···Si···O

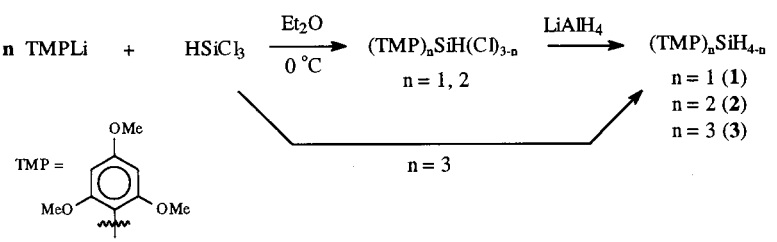


Scheme 1.

Table 1
Selected spectroscopic data, melting points, and elemental analyses for **1**–**3**

| | $^1$H-NMR ($\delta$, ppm) [a] | $^{29}$Si-NMR ($\delta$, ppm) [a] | IR ($\nu$, Si–H, cm$^{-1}$) [b] | m.p. (°C) | Elemental analysis |
|---|---|---|---|---|---|
| (TMP)$SiH_3$ (**1**) | 3.28 (s, *o*-$CH_3O$)<br>3.33 (s, *p*-$CH_3O$)<br>4.59 ($^1J_{Si-H}$ = 203 Hz)<br>6.00 (s, Ar–H) | −80.0 | 2192.0,<br>2155.1 | 52−54 | Calc.<br>C, 54.51; H, 7.12<br>Found<br>C, 54.53; H, 7.09 |
| $(TMP)_2SiH_2$ (**2**) | 3.35 (s, *o*-$CH_3O$)<br>3.36 (s, *p*-$CH_3O$)<br>5.61 ($^1J_{Si-H}$ = 208 Hz)<br>6.08 (s, Ar–H) | −67.6 | 2189.9,<br>2160.8 | 105–107 | Calc.<br>C, 59.31; H, 6.64<br>Found<br>C, 58.98; H, 6.51 |
| $(TMP)_3SiH$ (**3**) | 3.28 (s, *o*-$CH_3O$)<br>3.40 (s, *p*-$CH_3O$)<br>6.13 (s, Ar–H)<br>6.36 ($^1J_{Si-H}$ = 221 Hz) | −54.7 | 2169.0 | 172–174 | Calc.<br>C, 61.11; H, 6.46<br>Found<br>C, 61.06; H, 6.40 |

[a] $C_6D_6$; $^{13}$C-NMR and EI-MS data are found in Section 3.
[b] KBr pellet.

angles are listed in Table 3 and the structure refinement parameters and final residual values for **1**–**3** are listed in Table 4. Each compound exhibits approximately tetrahedral coordination at silicon. The Si–C bond distances for **1**–**3** are close to the mean value in the Cambridge Structural Database (CSD) for Si–aryl bonds found in a number of structures (1.88 Å, range 1.83–1.92). A CSD search on the general formula $ArSiH_3$ (Ar = aryl with any substituent) revealed six structures, 19 for $Ar_2SiH_2$, and 11 for $Ar_3SiH$. To our knowledge this is the first structural study for a homologous series of primary, secondary and tertiary silanes where the aryl groups remain the same.

A slight increase in the Si–C bond distance is observed when going from **1** (1.863 (2) Å) to **3** [1.870 (4)–1.880 (3) Å], possibly due to the increased steric hindrance of three aryl groups. The C–Si–C bond angles range from 109 to 115° in compounds **2** and **3** and are within the range observed for other secondary and tertiary silanes. For example, bis(8-(dimethylamino)-naphthyl)silane [13] displays a C–Si–C angle of 108° and the related tertiary silane, tris(8-(dimethylamino)-naphthyl)silane [14] exhibits three different C–Si–C angles in the range of 105–108°. Examination of the unit cells for **1**–**3** shows notable π-stacking of the aryl groups. In addition, a propeller arrangement of the aryl groups in **3** can be seen from Fig. 3. This arrangement is also found in other triarylsilane structures such as tris(8-(dimethylamino)naphthyl)silane, [14] tris(2-(dimethylamino)phenyl)silane, [15] and triphenylsilane [16].

Compounds **1**–**3** exhibit short intramolecular distances between silicon and the oxygen atoms in the *ortho*-methoxy groups. Fig. 4 shows the local environment at silicon for compounds **1**–**3**, and the nonbonded Si···O distances, respectively (covalent bonds are shown by solid lines and nonbonding interactions are designated by a dashed line). The Si···O separations are all shorter than the sum of the van der Waal's radii (3.62 Å) [17] but significantly longer than a typical covalent Si–O distance (1.67 Å) [18]. The Si···O distances in **1**–**3** all fall in the range of 2.86–3.13 Å. Each (TMP) ligand attached to silicon exhibits one short and one longer Si···O interaction from the *ortho*-OMe groups with O atoms roughly over faces or edges. A similar trend was seen in the structures of $(R_F)_2Si(H)F$ [2] and $(R_F)_2SiF_2$ [2,19] where fluorines from the *ortho*-$CF_3$ groups on the aryl ring were found to exhibit short intramolecular interactions with the silicon center. Each fluorine was found to occupy a face of the tetrahedron resulting in a (4 + 4) coordination environment, which approaches a distorted tetracapped tetrahedron, similar to bis[2,6-(dimethylaminomethyl)]silane [20]. Each aryl group displayed one short and one longer Si···F separation from

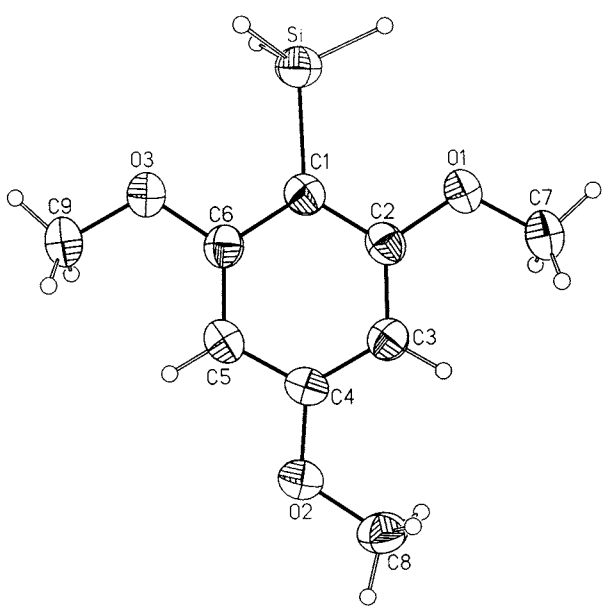


Fig. 1. Molecular structure of (TMP)$SiH_3$ (**1**) showing the atom-labeling scheme and 50% thermal ellipsoids.

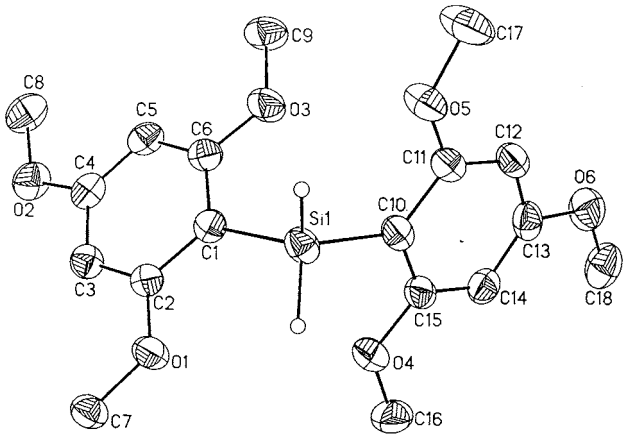


Fig. 2. Molecular structure of $(TMP)_2SiH_2$ (**2**) showing the atom-labeling scheme and 50% thermal ellipsoids.

one fluorine at each *o*-$CF_3$ group, analogous to the trend seen in the current study. In addition, short intramolecular E···F interactions were found in divalent $E(R_F)_2$ compounds (E = Ge, Sn, Pb) [21], in $(R_F)_2M$–$M(R_F)_2$ and $(R_F)_3M$ (M = In, Ga) [22].

The bond angles at the oxygen atoms in the *ortho*-OMe groups in **1**–**3** might suggest that they are pulled in towards the silicon atoms (see Table 2), however, the same trend in the angles is seen for the *para*-OMe substituents. In addition, little change is observed in the Si···O and Si–H distances in **1**–**3**. If significant extended coordination were present the Si···O and Si–H distances would be expected to lengthen through the sequence **1**–**3**. Therefore, it is unlikely that the shortened intramolecular Si···O distances in **1**–**3** involves a direct interaction but is probably due to constraints of the TMP ligand itself.

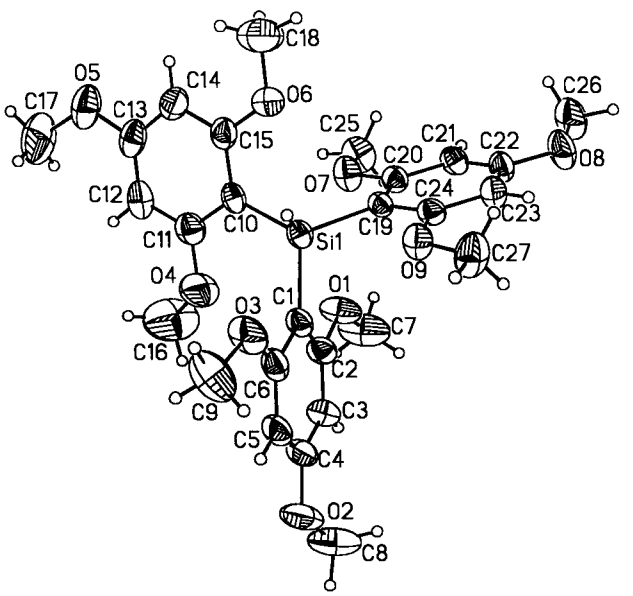


Fig. 3. Molecular structure of $(TMP)_3SiH$ (**3**) showing the atom-labeling scheme and 50% thermal ellipsoids.

### 2.3. Conclusions

The syntheses of the bulky arylsilanes, $(TMP)_nSiH_{4-n}$ [$n = 1$ (**1**), 2 (**2**), or 3 (**3**); TMP = 2,4,6-trimethoxyphenyl] have been performed by coupling reactions using aryllithium reagents and trichlorosilane followed by reduction with lithium aluminum hydride. However, in the case of **1**, cleaner reaction mixtures were obtained from $SiCl_4$ and (TMP)Li. The arylsilanes were characterized by $^1$H-, $^{13}$C-, and $^{29}$Si-NMR spectroscopy, IR, MS, X-ray crystallography, and elemental analysis. The X-ray structures for compounds **1**–**3** reveal relatively short intramolecular distances between the oxygen atoms in the *ortho*-OMe groups on the aromatic ring and the silicon center. The crystallographic data suggests that there is no direct interaction and that the short Si···O distances are a consequence of the geometrical constraints of the TMP ligand. This is the first reported structural study of a homologous series of aryl–hydrosilanes. Further studies are planned to explore the utility of these silanes in oxidative addition reactions to electron rich metal centers and in some selected cases as precursors to multiply bonded silicon species.

## 3. Experimental

All reactions were performed under an Ar atmosphere using standard Schlenk techniques. Diethyl ether, THF (pre-distilled from $CaH_2$) and 1,2-dimethoxyethane (DME) were distilled over Na–benzophenone ketyl under $N_2$. Trichlorosilane and $SiCl_4$ were distilled over $K_2CO_3$ before use. Benzene-$d_6$ and $CDCl_3$ were obtained from Cambridge Isotopes Labs, Inc. and were used as received. 1,3,5-Trimethoxybenzene, *n*-butyllithium, and lithium aluminum hydride are commercially available and were used as received.

$^1$H-, $^{13}$C-, and $^{29}$Si-NMR spectra were obtained on a Bruker ARX-500 MHz NMR spectrometer at frequencies of 500, 125, and 99 MHz, respectively using a 5-mm BB tunable probe. Proton and carbon NMR spectra were referenced to benzene (7.15 and 128.00 ppm, respectively) and silicon spectra were referenced to external TMS (0 ppm).

Infrared data were collected on a Perkin–Elmer 1600 Series FT-IR. GC analyses were carried out on a Hewlett–Packard Series II 5890 gas chromatograph using a DB-5 capillary column and GC–MS data were collected on a Hewlett–Packard 5899A GC–MS equipped with a RTE-A data system. Melting points were obtained on an Electrothermal 9100 capillary melting point apparatus and are uncorrected. Microanalyses were performed by Schwarzkopf Microanalytical Laboratory (Woodside, NY) or Atlantic Microlab, Inc. (Norcross, GA). HR-MS (EI) data were obtained

Table 2
Selected bond distances and angles for **1**–**3**

| $(TMP)SiH_3$ (**1**) | | $(TMP)_2SiH_2$ (**2**) | | $(TMP)_3SiH$ (**3**) | |
|---|---|---|---|---|---|
| *Bond distances* (Å) | | | | | |
| Si–C1 | 1.863 (2) | Si–C1 | 1.869 (2) | Si–C1 | 1.870 (2) |
| | | Si–C10 | 1.869 (2) | Si–C10 | 1.877 (2) |
| | | | | Si–C19 | 1.880 (3) |
| Si–H1 | 1.39 (2) | Si–H1 | 1.389 | Si–H1 | 1.382 |
| Si–H2 | 1.40 (3) | Si–H2 | 1.404 | | |
| Si–H3 | 1.42 (3) | | | | |
| *Bond angles* (°) | | | | | |
| O1–C2–C1 | 115.4 (2) | O1–C2–C1 | 115.0 (2) | O1–C2–C1 | 113.5 (3) |
| O1–C2–C3 | 121.8 (2) | O1–C2–C3 | 123.1 (2) | O1–C2–C3 | 121.6 (4) |
| O3–C6–C1 | 114.4 (2) | O3–C6–C1 | 113.7 (2) | O3–C6–C1 | 114.9 (4) |
| O3–C6–C5 | 123.2 (2) | O3–C6–C5 | 123.0 (2) | O3–C6–C5 | 123.3 (4) |
| O2–C4–C5 | 114.7 (2) | O2–C4–C3 | 115.0 (2) | O2–C4–C5 | 115.5 (4) |
| O2–C4–C3 | 123.5 (2) | O2–C4–C5 | 123.6 (2) | O2–C4–C3 | 123.3 (5) |
| | | O4–C15–C10 | 114.0 (2) | O4–C11–C10 | 115.8 (4) |
| | | O4–C15–C14 | 122.6 (2) | O4–C11–C12 | 121.1 (4) |
| | | O5–C11–C10 | 115.3 (2) | O5–C13–C14 | 115.7 (5) |
| | | O5–C11–C12 | 122.3 (2) | O5–C13–C12 | 123.3 (5) |
| | | O6–C13–C12 | 114.5 (2) | O6–C15–C10 | 113.8 (3) |
| | | O6–C13–C14 | 124.0 (2) | O6–C15–C14 | 122.9 (4) |
| | | | | O7–C20–C19 | 115.1 (3) |
| | | | | O7–C20–C21 | 122.6 (3) |
| | | | | O8–C22–C23 | 113.7 (3) |
| | | | | O8–C22–C21 | 124.3 (4) |
| | | | | O9–C24–C19 | 115.0 (3) |
| | | | | O9–C24–C23 | 121.2 (3) |
| | | C1–Si–C10 | 113.55 (8) | C1–Si–C10 | 112.5 |
| | | | | C10–Si–C19 | 115.3 |
| | | | | C1–Si–C19 | 109.3 |
| C1–Si–H1 | 112.0 (10) | C1–Si–H1 | 110.1 | C1–Si–H | 109.0 |
| C1–Si–H2 | 112.0 (11) | C1–Si–H2 | 109.4 | C10–Si–H | 103.0 |
| C1–Si–H3 | 110.7 (11) | C10–Si–H1 | 110.6 | C19–Si–H1 | 107.4 |
| | | C10–Si–H2 | 109.9 | | |
| H1–Si–H2 | 107 (2) | H1–Si–H2 | 102.8 | | |
| H1–Si–H3 | 110.0 (14) | | | | |
| H2–Si–H3 | 104 (2) | | | | |

from The Washington University High Resolution Mass Spectrometry Facility.

$^1$H- and $^{29}$Si-NMR, IR, m.p, and elemental analyses data for **1**–**3** are summarized in Table 1.

### 3.1. (2,4,6-Trimethoxyphenyl)silane, $(TMP)SiH_3$ (1)

To a solution of (TMP)H (5.4 g, 32 mmol) in 50 ml of THF was added *n*-butyllithium (14.1 ml, 2.5 M in hexanes) with rapid stirring over 10 min. After 2 h the solvent was removed in vacuo and the resulting off-white solid [(TMP)Li] was washed with 100 ml of pentane. A slurry of (TMP)Li in 80 ml of THF was added to a cooled solution ($-78$°C) of $SiCl_4$ (5.5 ml, 8.17 g, 48 mmol) in 50 ml of THF over 30 min. Several color changes were observed from bright pink initially to green then dark amber. After the addition was complete, the reaction mixture was warmed to r.t. and stirred overnight. The solvent was removed in vacuo, the solid dissolved in 50 ml of $Et_2O$ and then added dropwise to a slurry of $LiAlH_4$ (1.21 g, 32 mmol) in 75 ml of $Et_2O$. The reaction mixture was heated to reflux for 12 h. After an aqueous workup with saturated $NH_4Cl$, the organic layer was extracted with $Et_2O$ and dried over anhydrous $Na_2SO_4$. After removal of the solvent, the product was purified by Kugelrohr distillation and fractional crystallization providing a white solid (crude yield), 2.45 g, 45% (95% purity by GC). Attempts to remove the by-product (TMP)H by column chromatography and preparative GC failed. A pure sample of **1** was obtained by repeated fractional crystallization from pentane–$Et_2O$ (1:1). Spectroscopic data for **1**: $^{13}C\{^1H\}$-NMR ($C_6D_6$): $\delta$ 55.03 (*p*-OMe), 55.39 (*o*-OMe), 91.04 (*m*-ring carbon), 95.58 (*ipso*-carbon), 165.25 (*p*-ring carbon), 167.22 (*o*-ring carbon). MS (EI, 70 eV): $m/z$ 198 (100, $M^+$), 197 (31), 181 (11), 168 (17), 167 (39), 153 (12), 152 (25), 151 (34), 139 (24), 138 (26), 137 (74), 122 (16), 121 (64), 109 (14), 108 (21),

107 (24), 91 (48), 90 (11), 78 (14), 77 (17), 61 (16), 59 (63). HR-MS (EI, 70 eV): Anal Calc. for $C_9H_{14}O_3Si$ 198.0712; found, 198.0711.

### 3.2. 1-Deuterio-2,4,6-trimethoxybenzene, (TMP)D

Similar reactions of (TMP)H with *n*-BuLi to determine the percentage conversion to (TMP)Li were performed in THF, DME, and $Et_2O$ at r.t. or at reflux over 2–24 h. The conditions for maximum conversion are outlined in the typical experiment described below.

To a solution of (TMP)H (0.43 g, 2.56 mmol) in 20 ml of THF was added *n*-butyllithium (1.2 ml, 2.5 M in hexanes) with rapid stirring over 5 min. The reaction was stirred at r.t. for 2 h then $CD_3OD$ (0.16 ml, 3.94 mmol) was added over 6 min. After stirring for 1.5 h, 10 ml of $Et_2O$ were added. The volatiles were removed on a rotary evaporator, the remaining residue was extracted with hexanes (25 ml) and filtered to give a yellow solution. The hexane was evaporated and the residue was dissolved in $Et_2O$ and filtered. Upon removal of the solvent, (TMP)D was isolated as a white crystalline solid (0.25 g, 94%, m.p. 51–53°C, lit. [23] 51–53°C). Spectroscopic data for (TMP)D: $^1$H-NMR ($CDCl_3$): $\delta$ 3.75 (9 H, s, OMe), 6.08 (2 H, s, ArH). $^{13}C\{^1H\}$-NMR ($CDCl_3$): $\delta$ 55.13 ($OCH_3$), 92.50 (t, $^1J_{C-D} = 24.6$ Hz, C–D), 161.43 (multiplet, *C*–OMe). MS (EI, 70 eV): *m*/*z* 169 ($M^+$, 100), 168 (6), 140 (93), 139 (44), 126 (22), 125 (19), 110 (22), 109 (19), 108 (13), 96 (13), 95 (11), 80 (14), 79 (17), 78 (12), 69 (21), 53 (10).

### 3.3. Bis(2,4,6-trimethoxyphenyl)silane, $(TMP)_2SiH_2$ (2)

A solution of *n*-butyllithium (16 ml, 40 mmol, 2.5 M in hexanes) was added to (TMP)H (6.08 g, 36 mmol) in 65 ml of DME over 10 min. The reaction mixture was heated to reflux and stirred for 22 h. The resulting pale yellow slurry was added to $HSiCl_3$ (1.0 ml, 9.89 mmol) in 90 ml of DME over 45 min. The reaction mixture was stirred at r.t. for 24 h, the volatiles were removed on a rotary evaporator, and 90 ml of $Et_2O$ were added to the residue. To the mixture was added a slurry of $LiAlH_4$ (0.175g, 4.61 mmol) in 40 ml of $Et_2O$ over 20 min and the reaction mixture stirred for 24 h. After workup with saturated $NH_4Cl$ (50 ml), the organic layer was extracted with $Et_2O$, dried over anhydrous $MgSO_4$ then filtered to give a clear pale yellow solution. The solvent was removed on a rotary evaporator. Purification of $(TMP)_2SiH_2$ was achieved by silica gel column chromatography first with hexanes–$Et_2O$ (4:1) as the eluent (to remove any (TMP)H present) followed by $Et_2O$ to collect $(TMP)_2SiH_2$. White crystalline $(TMP)_2SiH_2$ (**2**) was obtained after removal of the solvent in 22% yield (0.84 g). No additional effort was made to optimize the yields. Spectroscopic data for **2**: $^{13}C\{^1H\}$-NMR($C_6D_6$): $\delta$ 54.68 (*p*-OMe), 55.30 (*o*-OMe), 91.09 (*m*-carbon ring), 102.01 (*ipso*-carbon), 164.06 (*p*-ring carbon), 166.99 (*o*-ring carbon). MS (EI, 70 eV): *m*/*z* 364 (19, $M^+$), 348 (13), 318 (18), 303 (11), 287 (17), 271 (10), 257 (10), 241 (11), 227 (21), 211 (10), 196 (100), 181 (19), 167 (96), 152 (38), 137 (38), 121 (58), 107 (12), 91 (21), 77 (13), 59 (48).

### 3.4. Tris(2,4,6-trimethoxyphenyl)silane, $(TMP)_3SiH$ (3)

To 2,4,6-trimethoxybenzene (7.93 g, 47.2 mmol) dissolved in 80 ml of DME, *n*-butyllithium (21 ml, 51.9 mmol, 2.5 M in hexanes) was added over 15 min followed by stirring at r.t for 3 h. A solution of $HSiCl_3$ (0.95 ml, 9.4 mmol) in 45 ml of DME was then added to the (TMP)H–*n*-BuLi solution over 10 min and the reaction mixture stirred at r.t. for 17 h. After aqueous

Table 3
Selected nonbonded distances and angles for **1**–**3**

| $(TMP)SiH_3$ (**1**) | | $(TMP)_2SiH_2$ (**2**) | | $(TMP)_3SiH$ (**3**) | |
|---|---|---|---|---|---|
| *Nonbonded angles* (°) | | | | | |
| O1···Si···O3 | 103.4 | O1···Si···O3 | 103.1 | O1···Si···O3 | 102.2 |
| | | O1···Si···O4 | 81.6 | O1···Si···O4 | 62.8 |
| | | O1···Si···O5 | 163.5 | O1···Si···O6 | 127.3 |
| | | O3···Si···O4 | 106.9 | O1···Si···O7 | 61.3 |
| | | O3···Si···O5 | 60.5 | O1···Si···O9 | 98.7 |
| | | O4···Si···O5 | 102.8 | O3···Si···O4 | 83.1 |
| | | | | O3···Si···O6 | 126.6 |
| | | | | O3···Si···O7 | 163.4 |
| | | | | O3···Si···O9 | 82.7 |
| | | | | O4···Si···O6 | 101.7 |
| | | | | O4···Si···O7 | 85.9 |
| | | | | O4···Si···O9 | 153.4 |
| | | | | O6···Si···O7 | 68.0 |
| | | | | O6···Si···O9 | 104.9 |
| | | | | O7···Si···O9 | 102.2 |

Table 4
Structure refinement parameters and final residual values for **1**–**3**

| | **1** | **2** | **3** |
|---|---|---|---|
| Formula | $C_9H_{14}O_3Si$ | $C_{18}H_{24}O_6Si$ | $C_{27}H_{34}O_9Si$ |
| Formula weight (amu) | 198.29 | 364.46 | 530.63 |
| Temperature (K) | 223 (2) | 213 (2) | 298 (2) |
| Crystal system | Monocliinic | Monocliinic | Monocliinic |
| Space group | $P2_1/n$ | $P2_1/c$ | $P2_1/n$ |
| Unit cell dimensions | | | |
| $a$ (Å) | 8.6072 (1) | 15.4221 (2) | 8.22610 (10) |
| $b$ (Å) | 11.3371 (2) | 16.5809 (2) | 24.6056 (3) |
| $c$ (Å) | 10.8916 (1) | 7.31360 (10) | 13.6607 (2) |
| $\alpha$ (°) | 90 | 90 | 90 |
| $\beta$ (°) | 95.824 (1) | 94.4770 (10) | 96.7760 (10) |
| $\gamma$ (°) | 90 | 90 | 90 |
| $V$ (Å$^3$) | 1057.32 (2) | 1864.47 (4) | 2745.72 (6) |
| $Z$ | 4 | 4 | 4 |
| $D_{calc.}$ (Mg m$^{-3}$) | 1.246 | 1.298 | 1.284 |
| Absorption coefficient (mm$^{-1}$) | 0.197 | 0.156 | 0.136 |
| Crystal size (mm) | $0.28 \times 0.22 \times 0.10$ | $0.42 \times 0.25 \times 0.15$ | $0.33 \times 0.20 \times 0.06$ |
| $\theta$ range for data collection (°) | 2.60–26.00 | 1.81–28.00 | 1.66–24.00 |
| Limiting indices | $-11 \le h \le 11$ | $-20 \le h \le 20$ | $-10 \le h \le 10$ |
| | $0 \le k \le 14$ | $-22 \le k \le 22$ | $-32 \le k \le 32$ |
| | $0 \le l \le 14$ | $-9 \le l \le 9$ | $-18 \le l \le 18$ |
| Reflections collected | 17 001 | 17 287 | 16 924 |
| Independent reflections | 2080 ($R_{int} = 0.08$) | 4480 ($R_{int} = 0.0555$) | 4312 ($R_{int} = 0.0897$) |
| Refinement method | Full-matrix least-squares on $F^2$ | Full-matrix least-squares on $F^2$ | Full-matrix least-squares on $F^2$ |
| Data/restraints/parameters | 2075/0/130 | 4467/0/234 | 4311/0/338 |
| Goodness-of-fit on $F^2$ | 1.026 | 1.068 | 1.113 |
| Final $R$ indices [$I > 2\sigma(I)$] | $R_1 = 0.0480$ | $R_1 = 0.0515$ | $R_1 = 0.0789$ |
| | $wR_2 = 0.1140$ | $wR_2 = 0.1106$ | $wR_2 = 0.1586$ |
| $R$ indices (all data) | $R_1 = 0.0818$ | $R_1 = 0.0821$ | $R_1 = 0.1201$ |
| | $wR_2 = 0.1312$ | $wR_2 = 0.1247$ | $wR_2 = 0.1778$ |
| Largest difference peak and hole (e Å$^{-3}$) | 0.230 and −0.247 | 0.400 and −0.212 | 0.349 and −0.293 |

workup with saturated $NH_4Cl$ (25 ml), the organic layer was extracted with $Et_2O$ and the organic layer separated and dried over anhydrous $MgSO_4$. The solution was filtered and the solvent was removed on a rotary evaporator. The residue was purified by silica gel column chromatography with first 1:3 hexane–ether as the eluent (to remove any (TMP)H present) followed by THF to collect $(TMP)_3SiH$. $(TMP)_3SiH$ was isolated as a white crystalline solid in 22% yield (1.09 g). Spectroscopic data for **3**: $^{13}C\{^1H\}$-NMR($C_6D_6$): $\delta$ 54.62 (*p*-OMe), 55.47 (*o*-OMe), 91.41 (*m*-ring carbon), 107.45 (*ipso*-ring carbon), 163.02 (*p*-ring carbon), 166.95 (*o*-ring carbon). MS (EI, 70 eV): $m/z$ 530 (0.4), 529 (0.5), 393 (41), 362 (100), 347 (20), 333 (14), 317 (14), 301 (17), 287 (11), 271 (11), 194 (11), 181 (10), 121 (11).

### 3.5. X-ray structural analysis of $(TMP)SiH_3$ (**1**), $(TMP)_2SiH_2$ (**2**), and $(TMP)_3SiH$ (**3**)

Crystals of appropriate dimensions were mounted on glass fibers in random orientations. Preliminary examinations and data collections were performed using a Bruker SMART Charge Coupled Device (CCD) Detector system single crystal X-ray diffractometer using graphite monochromated Mo–$K_\alpha$ radiation ($\lambda$ = 0.71073 Å) equipped with a sealed tube X-ray source. Preliminary unit cell constants were determined with a set of 45 narrow frames (0.3° in $\varpi$) scans. A typical data set consists of 4028 frames of intensity data collected with a frame width of 0.3° in $\varpi$ and counting time of 15 s/frame at a crystal to detector distance of 4.930 cm. The double-pass method of scanning was used to exclude any noise. The collected frames were integrated using an orientation matrix determined from the narrow frame scans. SMART and SAINT software packages [24] were used for data collection and data integration. Analysis of the integrated data did not show any decay. Final cell constants were determined by a global refinement of $xyz$ centroids of 8192 reflections. Collected data were corrected for systematic errors using SADABS [25] based upon the Laue symmetry using equivalent reflections.

Crystal data and intensity data collection parameters are listed in Table 4.

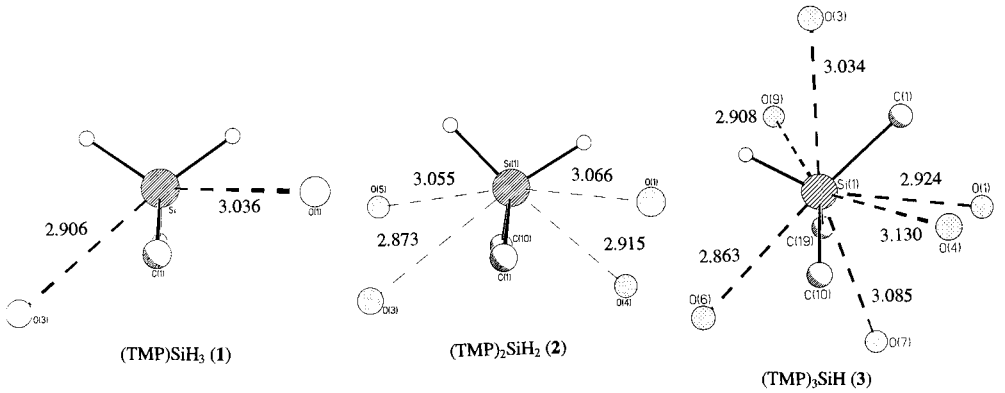


Fig. 4. Partial molecular structure of $(TMP)SiH_3$ (**1**), $(TMP)_2SiH_2$ (**2**), and $(TMP)_3SiH$ (**3**) showing the coordination environment around silicon with the atom-labeling scheme, and nonbonded Si···O distances (Å).

Structure solution and refinement were carried out using the SHELXTL-PLUS software package [26]. The structures were solved by direct methods and refined successfully in the space groups $P2_1/n$ for **1** and **3** and $P2_1/c$ for **2**. Full-matrix least-squares refinement was carried out by minimizing $\Sigma w(F_o^2 - F_c^2)^2$. The non-hydrogen atoms were refined anisotropically to convergence. The hydrogen atoms were treated using appropriate riding model (AFIX m3). The final residual values and relevant structure refinement parameters are listed in Table 4. Projection views of the molecules with non-hydrogen atoms represented by 50% probability ellipsoids and showing the atom labeling are presented in Figs. 1–3. Complete listings of the atomic coordinates, geometrical parameters and anisotropic displacement coefficients for the non-hydrogen atoms, positional and isotropic displacement coefficients for hydrogen atoms are deposited with the Cambridge Crystallographic Data Center (CCDC nos. 125736, 125737, 125738). A list of calculated and observed structure factors is available in electronic format.

## Acknowledgements

We thank the University of Missouri, St. Louis Research Award for financial support, the National Science Foundation and the University of Missouri, St. Louis Center for Molecular Electronics for equipment grants for The University of Missouri, St. Louis High Resolution NMR Facility and X-ray Crystallography Facility.

## References

[1] One of the first examples utilizing this approach was used for the preparation of the stable disilene, $Mes_2Si{=}SiMes_2$ (Mes = 2,4,6-trimethylphenyl); R. West, M.J. Fink, J. Michl, Science 214 (1981) 1343.
[2] J. Braddock-Wilking, M. Schiesher, L. Brammer, J. Huhmann, R. Shaltout, J. Organomet. Chem. 499 (1995) 89.
[3] For recent reviews on penta- and hexacoordinated silicon compounds see: (a) C. Chuit, R.J.P. Corriu, C. Reye, J.C. Young, Chem. Rev. 93 (1993) 1371. (b) R.R. Holmes, Chem. Rev. 90 (1990) 17.
[4] (a) J.Y. Corey, C.S. John, M.C. Ohmsted, L.S. Chang, J. Organomet. Chem. 394 (1986) 93. (b) A. Benouargha, D. Boulahia, B. Boutevin, G. Caporiccio, F. Guida-Pietrasanta, A. Ratsimihety, Phosphorus Sulfur Silicon 113 (1996) 79.
[5] J.Y. Corey, J. Braddock-Wilking, Chem. Rev. 99 (1999) 175.
[6] (a) T.D. Tilley, Comments Inorg. Chem. 10 (1990) 49. (b) J.Y. Corey, in: G. Larson (Ed.), Advances in Silicon Chemistry, vol. 1, JAI Press, Greenwich, CT, 1991, pp. 327.
[7] See for example: (a) F.T. Edelmann, Main Group Met. Chem. 17 (1994) 67. (b) F.T. Edelmann, Comments Inorg. Chem. 12 (1992) 259.
[8] (a) M. Wada, S. Higashizaki, A. Tsuboi, J. Chem. Res. (S) (1985) 38. (b) M. Wada, S. Higashizaki, J. Chem. Soc. Chem. Commun. (1984) 482.
[9] (a) G. Van Koten, A.J. Leusink, J.G. Noltes, J. Organomet. Chem. 85 (1975) 105. (b) A.J. Leusink, G. Van Koten, J.G. Noltes, J. Organomet. Chem. 56 (1973) 379. (c) F.A. Cotton, A.A. Koc, M. Millar, M. Inorg. Chem. 17 (1978) 2087.
[10] For a related example, see: H. Oehme, H. Weiss, J. Organomet. Chem. 319 (1987) C16.
[11] E.A. Williams, in: S. Patai, Z. Rappoport (Eds.), The Chemistry of Organic Silicon Compounds, vol. 8, Wiley, New York, 1989, pp. 511.
[12] THF was generally used due to the cost and ease of purification. The amount of (TMP)D formed (which represents the amount of (TMP)Li formed) was based on mass spectral data using the following equation: yield of $(TMP) = [P_D/(A + P_D)] \times 100\%$ where $P_D$ is the intensity of the parent ion for (TMP)D ($m/z$ = 169) and $A$ is the residual protonated (TMP)H material. The parameter $A$ is defined as: $A = (P-1)_D - (P-1)_H$ with the subscripts referring to the deuterated (D) or protonated (H) species. The $(P-1)$ term refers to the (parent ion − 1) peak in the mass spectrum.
[13] C. Brelier, F. Carre, R.J.P. Corriu, M. Poirier, G. Royo, J. Zwecker, Organometallics 8 (1989) 1831.
[14] C. Brelier, F. Carre, R.J.P. Corriu, G. Royo, M. Wong chi Man, Organometallics 13 (1994) 307.
[15] A. Kawachi, Y. Tanaka, K. Tamao, Organometallics 16 (1997) 5102.
[16] J. Allemand, R. Gerdil, Cryst. Struct. Commun. 8 (1979) 927.
[17] A. Bondi, J. Phys. Chem. 68 (1964) 441.
[18] G. Klebe, J. Organomet. Chem. 293 (1985) 147.

[19] J.-K. Buijink, M. Noltemeyer, F.T. Edelmann, J. Fluor. Chem. 61 (1993) 51.
[20] F. Carré, C. Chuit, R.J.P. Corriu, A. Mehdi, C. Reyé, Angew. Chem. Int. Ed. Engl. 33 (1994) 1097.
[21] (a) The divalent $Ge(R_F)_2$ compound was recently reported: J.E. Bender IV, M.M. Banaszak Holl, J.W. Kampf, Organometallics 17 (1998) 5166. (b) The corresponding tin and lead derivatives have also been prepared: H. Grützmacher, H. Pritzkow, F.T. Edelmann, Organometallics 10 (1991) 23. (c) S. Broker, J.-K. Buijink, F.T. Edelman, Organometallics 10 (1991) 25. (d) Recently, two compounds containing a Pb=Pb bond have been reported. One example utilizes the $R_F$ ligand: K.K. Klinkhammer, T.F. Fässler, H. Grützmacher, Angew. Chem. Int. Ed. Engl. 37 (1998) 124; and the other the 2,4,6-tris(triisopropylphenyl) substituent. (e) M. Stürmann, W. Saak, H. Marsmann, M. Weidenbruch, Angew. Chem. Int. Ed. Engl. 38 (1999) 187.
[22] R.D. Schluter, A.H. Cowley, D.A. Atwood, R.A. Jones, M.R. Bond, C.J. Carrano, J. Am. Chem. Soc. 115 (1993) 2070.
[23] Beilstein, fourth ed., 6(8) (1967) 6305.
[24] Bruker Analytical X-ray, Madison, WI, 1998.
[25] R.H. Blessing, Acta Crystallogr. A51 (1995) 33.
[26] G.M. Sheldrick, Bruker Analytical X-ray Division, Madison, WI, 1998.